«ФИЗИКА ЭЛЕМЕНТАРНЫХ ЧАСТИЦ И АТОМНОГО ЯДРА»
2000, ТОМ 31, ВЫП. 4

УДК 539.142.2; 539.144

THE NUCLEAR GIANT DIPOLE RESONANCE UNDER EXTREME CONDITIONS

M. Di Toro, V. Baran, M. Cabibbo**, M. Colonna,*

Laboratorio Nazionale del Sud, Via S. Sofia 44, I-95123 Catania,
and University of Catania, Italy

A.B. Larionov,

Dept.Theoretical Physics, Univ.Giessen, Germany,
I.V.Kurchatov Institute, Moscow, Russia

N. Tsoneva

INRNE, Sofia, Bulgaria

INTRODUCTION 876
A. Hot GDR 877
B. The Dynamical Dipole 878
HOT GDR: ZERO-TO-FIRST SOUND TRANSITION 878
RESPONSE FUNCTION AND ABSORPTION CROSS SECTION 881
Numerical results 882
GDR IN CHARGE ASYMMETRIC FUSION:
THE DYNAMICAL DIPOLE 888
THE INTERPLAY BETWEEN FUSION DYNAMICS
AND PRE-EQUILIBRIUM GDR 892
SUMMARY AND CONCLUSIONS 899
ACKNOWLEDGEMENTS 902
REFERENCES 902

*NIPNE, Bucharest, Romania
**CEA-SACLAY, France

«ФИЗИКА ЭЛЕМЕНТАРНЫХ ЧАСТИЦ И АТОМНОГО ЯДРА»
2000, ТОМ 31, ВЫП. 4

УДК 539.142.2; 539.144

THE NUCLEAR GIANT DIPOLE RESONANCE UNDER EXTREME CONDITIONS

M. Di Toro, V. Baran, M. Cabibbo**, M. Colonna,*

Laboratorio Nazionale del Sud, Via S. Sofia 44, I-95123 Catania,
and University of Catania, Italy

A.B. Larionov,

Dept.Theoretical Physics, Univ.Giessen, Germany,
I.V.Kurchatov Institute, Moscow, Russia

N. Tsoneva

INRNE, Sofia, Bulgaria

The isovector Giant Dipole Resonance (GDR) represents a well established collective motion of finite nuclei extensively studied since more than fifty years with fundamental contributions from the Dubna theory group lead by V.G.Soloviev. The dependence on the nuclear structure of the reference state, on top of which the collective mode is built, has already suggested its use in order to study nuclei far from the ground state. The time structure of the GDR mode actually allows a possibility of using it as a probe of nuclear systems very far from normal conditions. Here we report on properties of the GDR built on very exotic nuclear systems: i) high temperature, at the limit of the nuclear stability; ii) during charge equilibration in fusion dynamics. The isovector density wave propagation in symmetric nuclear matter (NM) at finite temperature is studied within the Landau–Vlasov theory. In cold NM a zero sound is found, which is changing to a first sound with increasing temperature. This transition, at variance to the case of a one-component Fermi liquid, does not result in the appearance of a maximum in the attenuation of the collective motion as a function of temperature. The damping width of a volume isovector mode is always monotonically increasing with temperature due to the presence of the collisional friction between neutron and proton liquids. However a clear effect of the transition is expected on the structure of the dipole response function. A transition temperature of about 4.5 MeV is deduced in heavy nuclei.

We describe the features of a direct GDR excitation in intermediate dinuclear systems with very exotic shape or charge distributions formed in particular fusion entrance channels (mass asymmetry $vs.$ charge asymmetry). We discuss the beam energy dependence of the effect due to the coupling between the pre-equilibrium dipole mode and other collective dynamical contributions. We derive some optimal entrance channel conditions to get this important pre-equilibrium cooling mechanism.

Изовекторный гигантский дипольный резонанс (ГДР) представляет собой хорошо известную коллективную моду движения конечной ядерной материи (ЯМ), которая активно изучалась в

*NIPNE, Bucharest, Romania
**CEA-SACLAY, France

течение более пятидесяти лет, и фундаментальный вклад в изучение которой внесла дубненская группа теоретиков под руководством В.Г.Соловьева. Зависимость данного состояния от ядерной структуры уже предполагает его использование для изучения ядер вдали от основного состояния. Временная структура ГДР-моды в действительности дает возможность ее использования в качестве зонда для изучения ядерных систем вдали от нормальных условий. В данном обзоре мы рассматриваем свойства ГДР, построенного на достаточно экзотических ядерных системах: а) при высоких температурах вблизи границы ядерной стабильности; б) в процессе установления зарядового равновесия при слиянии ядер. Распространение волн изовекторной плотности в симметричной ЯМ при конечной температуре изучается в рамках теории Ландау — Власова. В холодной ЯМ найден нулевой звук, который переходит в первый звук с увеличением температуры. Этот переход не имеет места для однокомпонентной ферми-жидкости из-за отсутствия максимума в затухании коллективного движения как функции температуры. Ширина затухания изовекторной моды всегда монотонно увеличивается с ростом температуры из-за наличия столкновительного трения между нейтронной и протонной жидкостями. Тем не менее ожидается выраженный переходный эффект в структуре дипольной функции отклика. Вычисленная температура перехода для тяжелых ядер — около 4,5 МэВ. Описываются особенности прямого возбуждения ГДР в промежуточной двухъядерной системе с достаточно экзотическим профилем или распределением заряда, формирующимся во входном канале слияния. Обсуждается зависимость эффектов от энергии пучка, возникающих благодаря наличию связи между предравновесной дипольной модой и другими коллективными динамическими вкладами. Определены некоторые оптимальные условия на входной канал для получения предравновесного охлаждающего механизма.

INTRODUCTION

The isovector giant dipole resonance represents a well established collective motion of finite nuclei extensively studied since more than fifty years [1]. The dependence on the nuclear structure of the reference state, on top of which the collective mode is built, has already suggested the use of GDR properties in order to study nuclei far from the ground state. The time structure of the GDR mode actually allows a possibility of using it as a probe of nuclear systems very far from normal conditions. We can roughly estimate an oscillation period of $\frac{2\pi\hbar}{E_{\rm GDR}} \simeq 80 - 100$ fm/c and a mean lifetime $\hbar/\Gamma_{\rm GDR} \simeq 50$ fm/c. Since the spreading width is the largest contribution to the total width $\Gamma_{\rm GDR}$ we can estimate around 50 fm/c also the time needed to build up the collective GDR mode in a Compound Nucleus (CN). All these time scales are relatively short and this makes the GDR an ideal probe to study nuclear systems under extreme conditions.

We investigate the properties of the GDR built on very exotic nuclear systems:

i) High temperature, at the limit of nuclear stability. We discuss first the problem of hot nuclei formation then we analyse the possibility of observation of a zero-to-first sound transition for the dipole propagation.

ii) Charge equilibration in fusion dynamics. We study the effect of a direct GDR excitation in intermediate dinuclear systems with exotic charge distributions, and shapes, formed in particular entrance channels (charge symmetry $vs.$ mass symmetry).

A. Hot GDR. With respect to temperature effects using a simple estimation for neutron evaporation with the Weisskopf formula [2] we can get a mean lifetime for heated compound nuclei ranging from 10^5 fm/c at $T = 1$ MeV to 50 fm/c at $T = 5$ MeV, so it seems possible to follow some GDR emission up to the stability limits of a hot CN.

The GDR γ emission has been extensively used to study the structure of excited nuclei, see the nice reviews [3, 4]. With increasing excitation energy the experimental results are however quite controversial, in particular on the temperature dependence of the GDR damping mechanisms, and so the evaluation of a limit temperature for the disappearing of the isovector dipole mode is still an open problem. Uncertainties in the data analysis are mostly coming from: i) hot nuclei formation (pre-equilibrium dynamical effects) [5–7, 9]; ii) statistical CASCADE calculations [8]; iii) subtraction of a direct bremsstrahlung component [9, 10]. The point i) is particularly delicate. The saturation of the GDR photon yield, observed in all experiments [11], can be indeed related to dynamical limits in thermal energy deposition on the detected heavy residue and not to a reduction of the GDR strength in hot nuclei. These pre-equilibrium effects seem to represent a serious intrinsic limitation to the use of fusion reactions to form hot nuclei. Inelastic α scattering experiments have given very nice data on heated nuclei, with smaller pre-equilibrium bias and less angular momentum effects [12, 13]. There is however an intrinsic limit on the reached excitation energy. New ways to form hot nuclei should be pursued.

Inelastic α scattering results clearly show a quite fast increase of the GDR damping with temperature in medium heavy nuclei (Sn, Pb). Two models, one based on the collisional damping and the other on shape fluctuations in an adiabatic picture, can reproduce this trend, see [8, 14]. The point we would like to stress here is that at $T \simeq 3$ MeV the width appears of the same order of the centroid energy and so we expect a disappearing of the GDR signal.

Recently the possibility of a transition from zero to first sound for the Giant Dipole propagation in hot nuclei has been suggested in order to allow a collective GDR emission from very excited nuclei [7, 15, 16]. This transition has been already clearly observed in other Fermi liquids, like ^{3}He [17].

Zero sound modes are mean field oscillations, quantum collective vibrations of the Fermi surface [18–20] while first sounds manifest as hydrodynamical waves. The damping mechanisms in the two regimes are quite different: mean field oscillations are relaxed by two-body collisions, collective modes due to local pressure variations by single particle escape from the flow. Consequently the temperature behaviour of the spreading width in Fermi liquids is just the opposite in the two cases: proportional to T^2 for zero sounds and to $1/T^2$, *i.e.*, following the mean free path, for first sounds. In case of a transition the expected saturation and eventual decrease of the attenuation could be the right mechanism to allow the GDR observation up to very high temperatures.

We remark that the possibility of such transition in hot nuclear systems has been recently suggested also for the fission mode [21–23] and in the hot fusion dynamics [24].

B. The Dynamical Dipole. Charge equilibration takes place on time scales of few units in 10^2 fm/c: in charge asymmetric entrance channels we expect to see a «direct dipole» collective excitation, with special dynamical features, which should give an extra yield to the photon spectrum in the GDR region. The idea is that we can form a fused dinuclear system with the charge not yet equilibrated and therefore with some extra dipole strength of nonstatistical nature. In this sense the «Dynamical Dipole» is a direct dipole contribution present in dissipative collisions initiated in charge asymmetric entrance channels. This new pre-equilibrium collective mode has been predicted some years ago [25, 26] and recently clearly observed in fusion [27–29] and deep-inelastic [30, 31] reactions. Some experiments have been performed also at intermediate energies, where other dynamical entrance channel features can be present [32, 33]. The appearance of this prompt dipole effect gives important information on the charge equilibration dynamics in connection to the reaction mechanism. A fully microscopic analysis is performed with quantitative predictions of the GDR photon yield based on a dynamics-statistics coupling model. Independent information on the damping of the dipole mode in very excited nuclear systems can be derived. Moreover the coupling between isovector dipole and large amplitude isoscalar monopole oscillations can be studied, of large interest also for the discussion on the fate of the GDR in hot nuclei. Since the effect is strongly dependent on fusion dynamics we study the beam energy variation of this extra dipole strength and we suggest some optimal conditions for the relative observation.

HOT GDR: ZERO-TO-FIRST SOUND TRANSITION

We show some predictions of a Landau Fermi Liquid approach [18,19,34–36] extended to isovector modes. This is correct in order to study the nuclear matter response, *i.e.*, to describe volume dipole modes of Steinwedel–Jensen (SJ) type. We insert finite nucleus effects just rescaling the wavelength of the normal modes. We expect this picture to have good physical grounds with increasing temperature due to the melting of shell structures and to the shorter nucleon mean free path which strongly reduces surface effects.

We find that the zero-to-first sound transition for isovector modes has quite relevant new features due to the presence of a counterstreaming flow between neutrons and protons, absent in other «one-component» Fermi liquids. As a consequence the effect of the transition on sound velocity and damping appears less dramatic but, none the less, still observable in the emitted photon spectra.

The starting point is the linearized kinetic equation for the variation of the isovector distribution function $\delta f_i = \delta f_p - \delta f_n$ taking into account the effect of collisions in a relaxation time approximation:

$$\frac{\partial \delta f_i}{\partial t} + \frac{\mathbf{p}}{m}\frac{\partial \delta f_i}{\partial \mathbf{r}} - \frac{\partial(\delta U_p - \delta U_n)}{\partial \mathbf{r}}\frac{\partial f^{(0)}_{n,p}}{\partial \mathbf{p}} = -\frac{(\delta f_i)_{l=1}}{\tau_1} - \frac{(\delta f_i)_{l\geq 2}}{\tau_2}, \qquad (1)$$

where the superscript (0) labels stationary values and δU_q is the dynamical component of the mean field potential. The unperturbed distribution function $f^{(0)}$ is in general the Fermi distribution at finite temperature. As self-consistent mean field potential we use a Skyrme-like form :

$$U_q = A\left(\frac{\rho}{\rho_0}\right) + B\left(\frac{\rho}{\rho_0}\right)^{\alpha+1} + C\left(\frac{\rho'}{\rho_0}\right)\tau_q, \qquad (2)$$

where $\rho = \rho_n + \rho_p$ and $\rho' = \rho_n - \rho_p$ are respectively the total (isoscalar) and the relative (isovector) density; $\rho_0 = 0.16$ fm^{-3} is the nuclear saturation density; $\tau_q = +1$ $(q = n)$, -1 $(q = p)$. The values of the parameters $A = -356.8$ MeV, $B = 303.9$ MeV, $\alpha = 1/6$ are adjusted to reproduce the saturation properties of symmetric nuclear matter, with a compressibility modulus $K = 201$ MeV. At saturation density the potential symmetry energy coefficient $C(\rho_0) = 32$ MeV satisfies the condition [16, 35]:

$$a_{\rm sym} = \frac{\epsilon_F}{3} + \frac{C(\rho_0)}{2} \ ,$$

where $a_{\rm sym} = 28$ MeV is the symmetry energy coefficient in the Weizsäcker mass formula and $\epsilon_F = 36$ MeV is the Fermi energy for symmetric nuclear matter at $\rho = \rho_0$.

On the right side of Eq. (1) $(\delta f_i)_l$ are distorsions of the local isovector d.f. having multipolarity l. We consider a generalization of the relaxation time method. In the case of isoscalar motion, when protons and neutrons are moving in phase, the conservation laws for particle number, momentum and energy will impose only multipolarities $l \geq 2$. However in the case of out-of-phase motion the effect of collisions is also to damp the isovector current, a process characterized by a relaxation time τ_1. The relaxation of higher order multipolarities is associated to an effective relaxation time τ_2. Following a standard procedure as described in [19, 36], one can derive from Eq. (1) a generalized dispersion relation for isovector sound in a two-component Fermi liquid [37, 38]:

$$\frac{s'}{s} + \chi(s)\left[F_0^{'} + \frac{is''}{s} + 3i\eta s''s'\right] = 0 \ , \qquad (3)$$

where

$$s' = \frac{\omega}{kv_F} \ , \quad s'' = \frac{1}{\tau_2 kv_F} \ , \quad s = s' + is'' \ , \quad \eta = 1 - \frac{\tau_2}{\tau_1} \ ,$$

$F_0^{'}$ is the isovector Landau parameter depending on the symmetry potential coefficient C: $F_0^{'} = 3C/(2\epsilon_F) = 1.33$ [16,35] and $\chi(s)$ is the Lindhard function [36]

$$\chi(s) = \frac{1}{2}\int_{-1}^{1} dx\, \frac{x}{x-s} = 1 - \frac{s}{2}\ln\left(\frac{s+1}{s-1}\right) .$$

The generalized dispersion relation Eq.(3) connects real and imaginary parts of the collective mode eigenfrequencies, $\omega = \omega_R + i\omega_I$, to the Landau parameter and the two relaxation times. It is useful to analyze two analytical limiting cases from where we get some insight regarding zero and first isovector sounds.

(i) *Zero-Sound Limit* ($\omega_R\tau_2 \gg 1$). Keeping only first order terms in the Taylor expansion of the Lindhard function we obtain the following set of equations:

$$\chi(s_0) = -\frac{1}{F_0^{'}} + O[(\frac{T}{\epsilon_F})^4] ,$$

$$-\omega_{I,zs} = \frac{1}{\tau_2}\left(1 - \frac{(s_0^2-1)(F_0^{'}+1+3s_0^2)}{F_0^{'}(F_0^{'}+1-s_0^2)}\right) + \frac{1}{\tau_1}\frac{3s_0^2(s_0^2-1)}{F_0^{'}(F_0^{'}+1-s_0^2)} ,$$

where $s_0 = \omega_{R,zs}/kv_F$ is the phase velocity of the zero sound in units of the Fermi velocity $v_F = 0.28c$. Since for Landau parameters of the order of unit we have solutions $s_0 \approx 1$, we conclude that at low temperatures the damping of zero sound is essentially due to the distortions with $l \geq 2$ and much less due to the friction of a relative motion. The collisional damping has a T^2 dependence, ruled by $1/\tau_2$, as in the case of the zero sound in one-component systems.

This zero sound collective motion is exactly the Steinwedel–Jensen (SJ) dipole volume mode. Indeed for a $F_0^{'} = 1.33$ we have a solution $s_0 = 1.08$. Since $\lambda = 4R$ is the maximum wavelength for a dipole volume oscillation in a finite nucleus of the radius $R = 1.2A^{1/3}$, we have a normal mode with the wave number $k = \pi/2R$ and so a collective energy $\hbar\omega = 1.08\hbar kv_F = 78.1A^{-1/3}$, typical of the SJ systematics, which well reproduces the g.s. GDR energies in heavy spherical nuclei [1].

(ii) *First-Sound Limit* ($\omega_R\tau_2 \ll 1$). In this case we have $|s| \gg 1$. Therefore, following Refs. 19, 36, we decompose the Lindhard function $\chi(s)$ in powers of $1/s$ and we finally get the following set of solutions for real and imaginary parts:

$$-\omega_{I,fs} = \frac{1}{2\tau_1} + \frac{2}{15}(kv_F)^2\tau_2 \approx \alpha T^2 + \beta\frac{k^2}{T^2} ,$$

$$\omega_{R,fs} = \sqrt{\omega_0^2 - \omega_{I,fs}^2} , \quad \omega_0 = kv_F\sqrt{\frac{1+F_0^{'}}{3}} .$$

Also in the first-sound regime we see a T^2 increase of the attenuation, now ruled by $1/\tau_1$. Therefore in presence of the transition in the isovector case we would expect just a change in the T^2 slope of the damping. The real part of the frequency is given by the two terms under square root. The first one, ω_0^2, is obtained in the hydrodynamical limit without any attenuation, Ref. 16. The second one, $-\omega_{I,fs}^2$, is coming mostly from the friction between counterstreaming proton and neutron liquids and leads to the disappearing of the mode at high temperature.

RESPONSE FUNCTION AND ABSORPTION CROSS SECTION

The correct way to compare theoretical predictions with experiments is to compute GDR strength functions at various temperatures to insert in statistical calculations [8] *at each step of the evaporation cascade* . In this scheme we will get not only centroid energies and FWHM (Full Width Half Maximum) but also a more detailed shape of the response function which is affecting the form of the γ-emission spectrum.

The density–density response function for a periodic in space and time isovector external field $\delta V_i = \delta V_p - \delta V_n \propto \exp(i\mathbf{kr} - i\omega t)$, Refs. 39–41, $\chi_{\rho\rho}(\omega, k) = = -\frac{2\delta\rho_i}{\delta V_i}$, can be evaluated in a Fermi liquid (see Refs. 34, 37, 38, 42) as

$$\chi_{\rho\rho}(\omega, k) = \frac{2N(T)\chi_T^\tau}{1 + F_0^{'}\chi_T^\tau} \ ,$$

where $N(T)$ is a density of states and we introduce the unperturbed response $\chi_T^\tau(\omega, k)$ which represents a kind of extended Lindhard function in the sense that the pole equation for the response function $1 + F_0^{'}\chi_T^\tau(\omega, k) = 0$ leads to the previous expression for dispersion relations, Eq. (3).

The dipole strength function per unit volume is given by $S(\omega, k) = \frac{1}{\pi}\mathrm{Im}(\chi_{\rho\rho})$, and the photoabsorption cross section in a thermally excited nucleus, to use in cascade calculations, can be expressed as [34, 42, 43]:

$$\sigma_{abs}(\hbar\omega) = \frac{4\pi^2 e^2}{\hbar c k^2 \rho_0}\frac{NZ}{A}\hbar\omega S_k(\omega) \ .$$

In the following we will compare predictions for the temperature behaviour of GDR strength functions in $^{208}\mathrm{Pb}$ (wavenumber $k = \pi/2R_{\mathrm{Pb}} = .22$ fm^{-1}).

In the first sound limit the γ-absorption cross section has a simple analytical form. Indeed from the decomposition of the Lindhard function it is straightforward to obtain a Lorentzian structure :

$$\sigma_{abs}(E_\gamma) \simeq \frac{4\pi e^2\hbar}{mc}\frac{NZ}{A}\frac{\Gamma E_\gamma^2}{(E_\gamma^2 - E_0^2)^2 + \Gamma^2 E_\gamma^2} \ .$$

The centroid energy E_0 and the width Γ are related to the first sound frequency ω_0 and to the damping rate $-\omega_{I,fs}$ $E_0 = \hbar\omega_0$, $\Gamma = -2\hbar\omega_{I,fs}$. This result, which confirms previous macroscopic predictions [44], is important since it will represent a good experimental signature of the occurred transition.

Numerical results. From the previous discussions we can conclude that the transition from zero to first sound for isovector modes is dictated by the relative values of the relaxation times corresponding respectively to the $l = 1$ and $l = 2$ multipolarities. In turn the latter are depending on the kinematic factors related to the type of deformation in momentum space and to the nucleon–nucleon (NN) cross sections and their isospin dependence. Indeed while in the $l = 1$ case we have only σ_{np} contributions, in the $l = 2$ we have all possible nn, pp and np combinations, although with different kinematical factors. We expect a τ_1 in general larger than τ_2 and then the possibility of observation of the zero-to-first sound transition. We have a general structure

$$\frac{1}{\tau_l} = -\frac{\int d^3\mathbf{p} P_l(\cos\theta)\delta I}{\int d^3\mathbf{p} P_l(\cos\theta)\delta f} \equiv \frac{T^2}{\kappa_l}.$$

Memory effects can be taken into account following the Landau prescription, *i.e.*, by the change $\tau_{\rm BUU} \to \tau_{\rm BUU}/(1 + (\hbar\omega_R/2\pi T)^2)$, where $\tau_{\rm BUU}$ is the relaxation time derived from Boltzmann–Uehling–Uhlenbeck collision integral and $\hbar\omega_R$ is the resonance energy. Analytical derivations can be found in many Refs. 45–47. We have followed the detailed calculation of Ref. 38.

We will use here three sets of isovector relaxation time parameters $(\kappa_1;\kappa_2)$. Set 1 is found from vacuum NN cross sections: $(\kappa_1;\kappa_2) = (503; 491)$ MeV^2 fm/c. Set 2 corresponds to in-medium cross sections, reduced following the prescription of Ref. 48 calculated at normal nuclear density in cold nuclear matter: $(\kappa_1;\kappa_2) = (1123; 1068)$ MeV^2 fm/c. Set 3 is obtained from Set 1 just multiplying by a factor 10 the relaxation time τ_2 of the quadrupole Fermi surface distortions: $(\kappa_1;\kappa_2) = (503; 4910)$ MeV^2 fm/c. Set 3 is adopted to study the structure of the response function, and corresponding effects on dipole emission, in a case where we cannot have the zero-to-first sound transition.

In Fig. 1 (solid lines) we show a photoabsorption cross section $\sigma_{abs}(\hbar\omega)$ calculated at various temperatures for a nucleus ^{208}Pb with Set 1 of relaxation times (vacuum NN cross sections). The centroid energy E_0 is slightly decreasing and the width Γ is increasing strongly as the temperature grows. The transition is accompanied by a Lorentzian shape restoration. The transition is nicely seen in Fig. 2 where the temperature dependence of the GDR widths is presented, calculated with the various Sets of relaxation times: solid lines show the FWHM from the full numerical calculation of the photoabsorption cross section; long-dashed lines, from the Lorentzian of the hydrodynamic limit; and finally short-dashed lines are imaginary (multiplied by -2) parts of the frequency in the zero-sound limit.

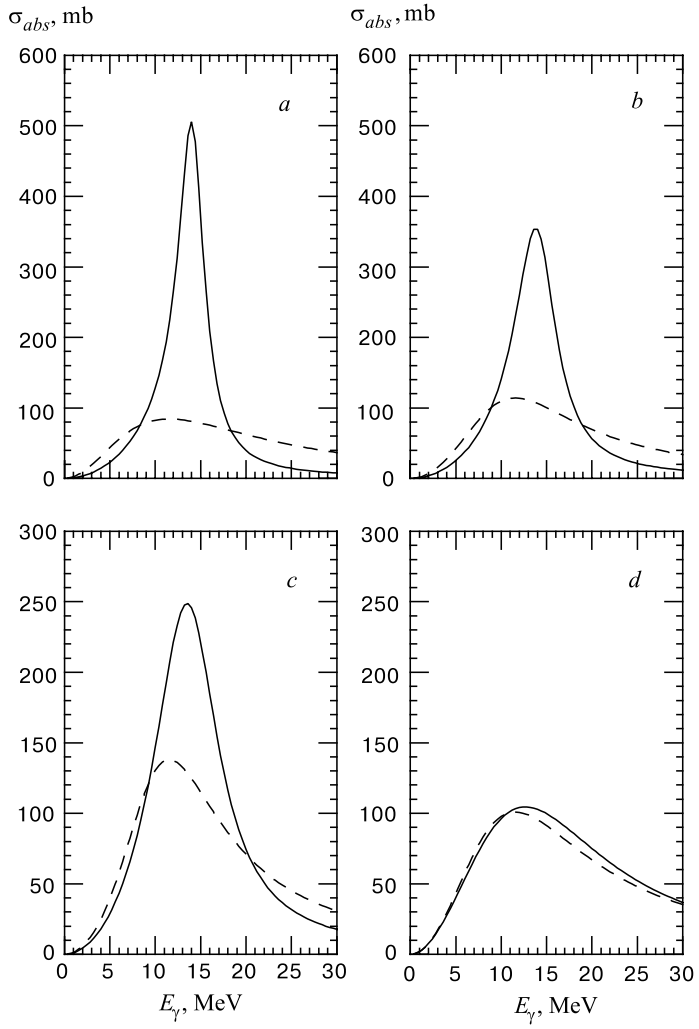

Fig. 1. Photoabsorption cross section by $^{208}\mathrm{Pb}$ calculated with Set 1 of relaxation times at different temperatures. Solid lines — full calculation. Dashed lines — Lorentzians obtained in hydrodynamic limit. a) to d): $T = 1, 2, 3, 6$ MeV, respectively

With the free cross sections (Set 1, Fig. 2*a*) at small and moderate temperature $T \leq 4$ MeV the zero-sound solution describes very well the temperature dependence of the FWHM. The hydrodynamic first-sound regime starts at high temperatures $T \geq 5.5$ MeV and exists up to $T_{\max} \simeq 7$ MeV, when the collective mode vanishes in presence of a too large counterstreaming friction. One

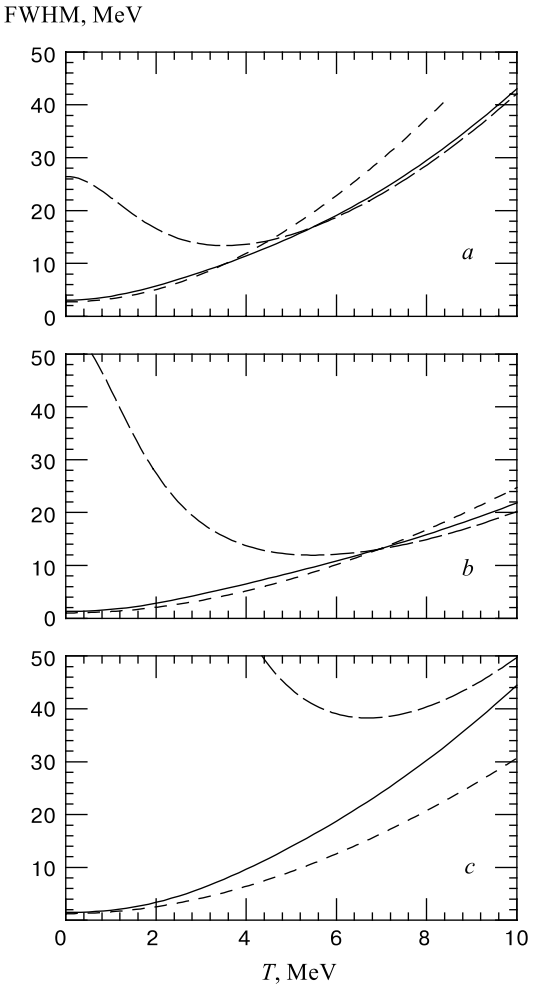

Fig. 2. Temperature dependence of the GDR width in $^{208}\mathrm{Pb}$ calculated with Set 1 (panel *a*), Set 2 (*b*) and Set 3 (*c*). Solid lines — FWHM of the full photoabsorption cross section. Short-dashed lines — the doubled absolute value of the imaginary part of the zero-sound frequency $2\hbar|\omega_{I,zs}|$. Long-dashed lines — FWHM of the first-sound Lorentzian $\Gamma = 2\hbar|\omega_{I,fs}|$

can fix then a transition temperature $T_{tr} \simeq 4.5$ MeV at the cross point of the zero and first sound solutions. This value, in agreement with earlier evaluations (Refs. 7, 46, 16), appears to be quite high to be reached experimentally. However we can expect to see some signatures also at lower temperatures due to the changes in the shape of the response function (see Fig. 1).

The calculation with Set 2 (in-medium reduced cross sections) gives qualitatively the same results. Now the transition temperature is higher : $T_{\rm tr} \simeq 7$ MeV (see Fig. 2*b*). Finally with Set 3, as expected, we don't see any transition in a realistic range of temperatures (see Fig. 2*c*).

As is already stressed the aim of this work is to show that signatures of the zero-to-first sound transition can be eventually seen in experimental γ-decay spectra from heated nuclei. Until recent times only a theoretical width of hot GDR defined as the FWHM of calculated photoabsorption strength has been compared to the FWHM extracted from a statistical model fit to the experimental γ spectrum using a *Lorentzian photoabsorption strength with a fixed* $\Gamma_{\rm GDR}$ *value*. The shape of the theoretical strength distribution has been neglected in this comparison. In Ref. 8, the first direct use of the theoretical strength functions into the statistical code CASCADE has been performed. This analysis has revealed the importance of the strength shape for a detailed description of the γ spectrum. A particular collisional damping model calculations have been used in Ref. 8 and only for a ^{120}Sn nucleus. The strength functions of daughter nuclei, produced mostly by the neutron emission, have not been taken into account. In the present work we implement the approach using the photoabsorption strengths, calculated above within different prescriptions, at each step of the deexcitation chain. We use a Monte-Carlo approach, the statistical code MONTECASCA of Ref. 49, 50. The temperature T of each nucleus in the chain is calculated as $T = \sqrt{E^*/a}$, where $a = A/8$ MeV^{-1} is the level density parameter, E^* and A are respectively the excitation energy and the mass number.

We have performed calculations of the γ spectra from a nucleus ^{208}Pb at two initial excitation energies $E^* = 45$ and 100 MeV, where nice data are available from inelastic $\alpha-$scattering experiments (see [13] and refs. therein). A bremsstrahlung contribution of the kind $Y_{b.s.}(E_\gamma) = A_{b.s.} \exp(-E_\gamma/T_{b.s.})$, where $T_{b.s.} = 14$ MeV, normalized to γ yield in the energy region of 20–25 MeV, as suggested in the experimental papers, has been subtracted before the comparison to theory predictions.

The results are shown in Fig. 3. The calculation with Set 1 (vacuum cross sections, solid lines) gives the best overall agreement with the data. Set 2 (in-medium reduced cross sections, short-dashed lines) produces too small GDR widths (see also Fig. 4).

The role of a damping of Fermi surface distortions with multipolarity $l \geq 2$, and related presence of a transition to first sound, can be seen from the comparison of the spectra given by Set 1 and Set 3 (long-dashed lines). The presence in Set 3 of a damping of almost only $l = 1$ distortions is clearly not enough to describe the γ spectra. The reason is again in too small widths for low temperatures $T \leq 3$ MeV (see also Fig. 4). We remark that roughly Set 3 simulates the collisional damping of a Goldhaber–Teller GDR mode ([43] and refs. therein), picture based on the relative motion of the two rigid subsystems

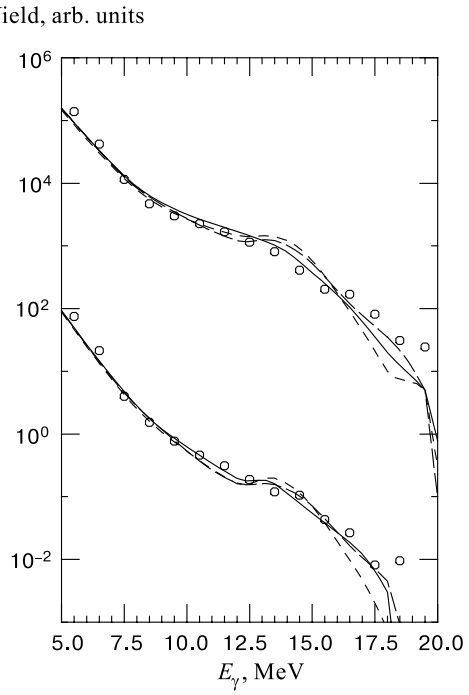

Fig. 3. γ yield as a function of the energy E_γ from ^{208}Pb at $E^* = 45$ MeV (theory), 40–50 MeV (experiment) — lower curves and circles, and at $E^* = 100$ MeV (theory), 100–110 MeV (experiment) — upper curves and circles. Solid, short-dashed and long-dashed lines correspond to the calculations with Set 1, 2 and 3. Circles show the data from Ref. 13 after subtraction of the bremsstrahlung component

of protons and neutrons with, evidently, only the $l = 1$ damping (see also the discussion in Ref. 45).

A better understanding of the discrepancies between theory and experiment is reached when we look at the γ spectra on a linear scale. In Fig. 4*a,b* the modified spectra (see Ref. 51) obtained by subtraction of the low $\gamma-$energy statistical contribution are presented. At $E_\gamma \simeq E_{\rm GDR} = 10 - 15$ MeV, all the discrepancies present in Fig. 3 are much better visible in the modified spectra. In fact, it is seen from Fig. 4*a,b*, that Sets 2 and 3 give modified yields shifted to higher energies E_γ, and narrower, with respect to Set 1 and the data.

Finally in Fig. 5 we report the centroid energies E_0 and widths FWHM of the photoabsorption cross section *vs.* T for the various choices of relaxation times.

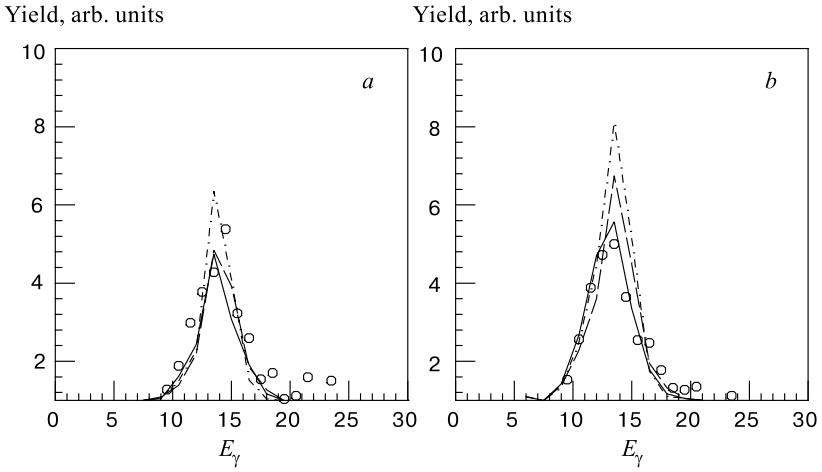

Fig. 4. Comparison of subtracted γ yield (see text). Panel a — $E^* = 45$ MeV (theory), 40–50 MeV (experiment). Panel b — $E^* = 100$ MeV (theory), 100–110 MeV (experiment). Notations are the same like in Fig. 3

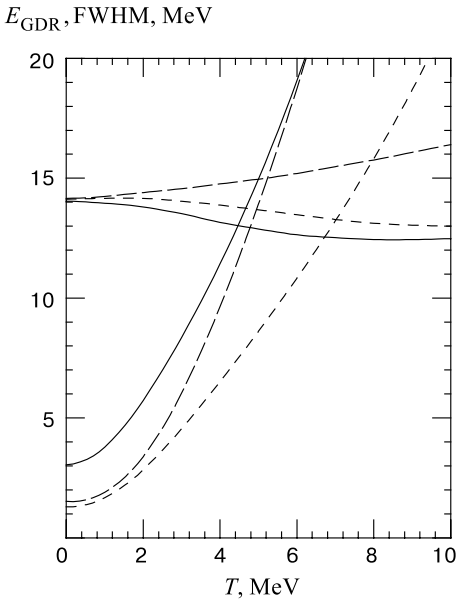

Fig. 5. Temperature dependence of the GDR centroid energy E_0 — upper curves and FWHM — lower curves in $^{208}\mathrm{Pb}$ calculated from the full photoabsorption cross section. Notation of lines is the same like in Fig.3

GDR IN CHARGE ASYMMETRIC FUSION: THE DYNAMICAL DIPOLE

Fusion processes in charge asymmetric entrance channels give a clear example on how emitted GDR photons may carry information on a Compound Nucleus (CN), formed during the reaction dynamics, very far from normal conditions.

In dissipative collisions energy and angular momenta are quickly distributed among all single particle degrees of freedom while charge equilibration takes place on larger time scales [52]. Therefore for charge asymmetric entrance channels at the time of CN formation we can easily have some relic of a pre-equilibrium GDR from dipole oscillations in the isospin transfer dynamics [26]. The result will be an enhanced GDR-photon emission with special features due to the nonstatistical nature of this extra contribution.

An enhancement of the GDR gamma ray yield has been observed experimentally in fusion reaction between heavy ions with different neutron-to-proton ratios. Flibotte et al. [27], in collision between $^{40}\mathrm{Ca}$ $(N/Z = 1)$ and $^{100}\mathrm{Mo}$, $(N/Z = 1.38)$, at 4 A MeV beam energy, producing a CN at 70 MeV excitation energy, counted a number of emitted GDR photons over the whole cascade 16% larger than in the case when the same CN was formed with a symmetric N/Z combination. Similar effect has been observed by Cinausero et al. [28]: an increase of 36% resulted when they compared GDR-photon yields from a CN populated at 110 MeV excitation energy via the reactions $^{16}\mathrm{O}$ $(N/Z = 1)$ + + $^{98}\mathrm{Mo}$ $(N/Z = 1.33)$ and $^{50}\mathrm{Ti}$ $(N/Z = 1.18)$ + $^{64}\mathrm{Ni}$ $(N/Z = 1.28)$, respectively. Some experiments have been performed also at intermediate energies [32,33] and in Deep Inelastic Collisions [30], where other dynamical effects may be present.

In fact, theoretically, an extra-yield of gamma rays was predicted some years ago by Chomaz et al., [25,26], in a simple model of a GDR-phonon gas interacting with the CN. The essential quantity in this approach is the mean number of excited GDR-phonons at the time when a CN is formed, $n^{(0)}_{\mathrm{GDR}}$. The emission of GDR photons is enhanced if $n^{(0)}_{\mathrm{GDR}}$ is greater than the value corresponding to statistical equilibrium between GDR oscillator and CN heat bath. The N/Z asymmetry of colliding heavy ions will trigger in the early stage of the reaction — the charge equilibration process. Several experiments and realistic simulations have indicated that the related dipole oscillation has the characteristics of a GDR-type quantal collective motion [52–57]. Expressed in terms of Brink–Axel hypothesis [58] this means that a GDR may be built not only on equilibrium states, of a warm nucleus for example, but also on nonequilibrium states during the CN formation phase. $n^{(0)}_{\mathrm{GDR}}$ represents the number of phonons in this mode at the time of a CN formation t_{CN}.

Although it was assumed that the quantity $n^{(0)}_{\mathrm{GDR}}$ is intimately related to the presence of pre-equilibrium effects, the way it is determined and affected by the

projectile target N/Z asymmetry and entrance-channel dynamics has not been investigated yet. From the previous discussion we clearly distinguish three main phases in the entrance-channel dynamics: *I.* The approaching phase, with the two partners still keeping their own response properties; *II.* The dinuclear phase, with relative collective response; *III.* The CN formation. We will call $t = 0$ the starting time of the phase *II*, *i.e.*, the onset of the main dissipation mechanisms, including the charge equilibration. In this phase a pre-equilibrium dipole mode is present damped with a spreading width $\Gamma^{\downarrow} \equiv \hbar\mu(t)$, where the time dependence is expressing a nonequilibrium situation. The correspondent number of phonons will show an exponential decrease

$$n(t) = n_i e^{-\int_0^t \mu(t)dt}, \tag{4}$$

where n_i is the number of phonons at the moment when charge equilibration begins. Fusion experiments seem to indicate that this will happen once the decision for fusion is taken [52]. This means that when the system passes from the strong absorption configuration through the barrier, the neck is large enough to allow for an isospin collective motion. Therefore we can assume that the configuration reached soon after, when the interdistance between the center of mass of the two nuclei is around the sum of their radii, represents the starting point of the collective pre-equilibrium GDR mode. Ii is important to stress that at this moment we have already reached a quite noticeable density overlap and therefore the considered configuration is not corresponding to the naive picture of the two nuclei as two touching rigid spheres. This will become clear from density contour plots and collective behaviours we will show later in microscopic dynamical simulations.

In order to estimate n_i we consider a harmonic oscillator description for the GDR:

$$H_{\mathrm{GDR}}(t) = \frac{\Pi^2(t)}{2M} + \frac{M\omega^2(t)}{2}X^2(t), \tag{5}$$

where $M = \frac{ZN}{(Z+N)}m$ is the reduced mass of the neutron–proton relative motion, $m = 935$ MeV being the nucleon mass, $N = N_1 + N_2$, ($Z = Z_1 + Z_2$), the total number of neutrons (protons). Here Π denotes the relative momentum:

$$\Pi = \frac{NZ}{A}\left(\frac{P_p}{Z} - \frac{P_n}{N}\right) \tag{6}$$

with P_p (P_n) the centre of mass momentum for protons (neutrons) while $X = R_p - R_n$ is the distance between the centres of mass of the two components. The initial number of phonons is defined as:

$$n_i = \frac{H_{\mathrm{GDR}}(0)}{\hbar\omega(0)} \approx \frac{1}{2\hbar^2}M(\hbar\omega(0))X^2(0) \tag{7}$$

if we neglect the kinetic part contribution. We expect this approximation not to work at higher incident beam energies, as discussed later. Here $X(0)$ has the following expression:

$$X(0) = \frac{Z_1 Z_2}{A}(\frac{N_1}{Z_1} - \frac{N_2}{Z_2})(R_1 + R_2). \tag{8}$$

We can consider for the initial elongated shape a phonon energy [43]:

$$\hbar\omega(0) = \frac{R}{R_1 + R_2} E_{\mathrm{GDR}}, \tag{9}$$

where $R = r_0 A^{1/3}$, ($r_0 = 1.2$), is the equilibrium radius of the CN and $E_{\mathrm{GDR}} \simeq$ $\simeq 78 A^{-1/3}$ is the energy of a phonon built on CN, corresponding to the centroid of GDR spectrum in medium-heavy nuclei.

In conclusion we can finaly express the mean number of phonons at the time when a CN is formed as:

$$\begin{aligned} n^{(0)}_{\mathrm{GDR}} = n(t_{\mathrm{CN}}) \approx \frac{1}{2\hbar^2} M R (R_1 + R_2) \frac{Z_1^2 Z_2^2}{N^2 Z^2} \times \\ \times \left(\frac{N_1}{Z_1} - \frac{N_2}{Z_2}\right)^2 E_{\mathrm{GDR}} \exp\left(-\mu_{\mathrm{ave}} t_{\mathrm{CN}}\right) = \\ = 1.4 \frac{(A_1^{1/3} + A_2^{1/3})}{A} \frac{Z_1^2 Z_2^2}{NZ} \left(\frac{N_1}{Z_1} - \frac{N_2}{Z_2}\right)^2 \exp\left(-\mu_{\mathrm{ave}} t_{\mathrm{CN}}\right), \end{aligned} \tag{10}$$

where μ_{ave} is an average value of the spreading width:

$$\mu_{\mathrm{ave}} = \frac{1}{t_{\mathrm{CN}}} \int_0^{t_{\mathrm{CN}}} \mu(t) dt. \tag{11}$$

We observe that $n^{(0)}_{\mathrm{GDR}}$ will depend critically on fusion dynamics (through the time scale for Compound Nucleus formation) as well as on properties of the spreading width $\mu(t)$.

After the time t_{CN} we have to switch to the approach introduced in [26] for the CN decay phase. The number of GDR-phonons is still time-dependent since charge equilibration is still going on, but now we can have some feeding from the CN heat bath with a width $\Gamma_{\mathrm{feed}} \equiv \hbar\lambda$. The result is [26] (now the origin of time is t_{CN}):

$$n_{\mathrm{GDR}}(t) = \frac{\lambda}{\mu}\Big[1 - (1 - n^{(0)}_{\mathrm{GDR}} \frac{\mu}{\lambda}) \exp\left(-\mu t\right)\Big] \tag{12}$$

which asymptotically leads to the statistical value

$$\frac{\lambda}{\mu} = \frac{\rho(E^* - E_{\mathrm{GDR}})}{\rho(E^*)} \approx \exp\left(-E_{\mathrm{GDR}}/T\right), \tag{13}$$

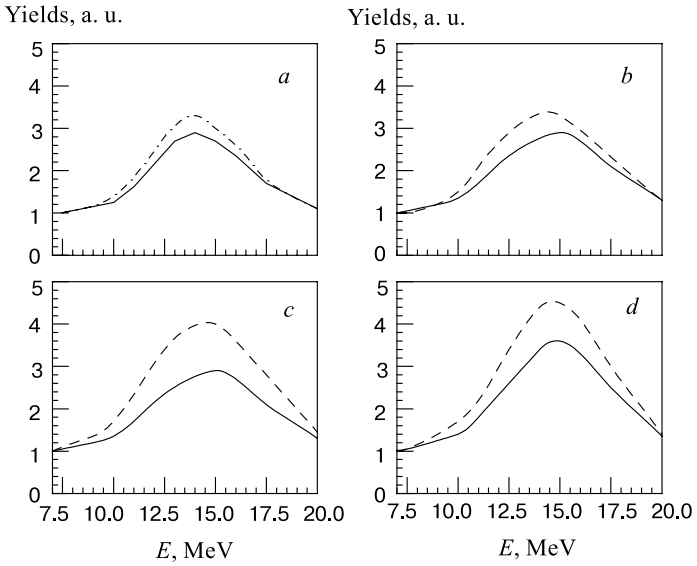

Fig. 6. Subtracted γ spectra from a $^{140}\mathrm{Sm}$ CN formed at $E^* = 71$ MeV in the charge asymmetric ($\mathrm{Ca} + \mathrm{Mo}$ — dashed lines) and symmetric ($\mathrm{S} + \mathrm{Pd}$ — solid lines) entrance channel: a) Experiment [27]; b), c), d), simulations (see text) with $(n^{(0)}_{\mathrm{GDR}}, \Gamma^{\downarrow})$ respectively equal to (0.14, 8 MeV), (0.6, 8 MeV), (0.14, 4.8 MeV). 10^5 Montecarlo events

where $\rho(E)$ is the level density, E^* is the CN excitation energy and T the corresponding temperature. From this discussion we see that the quantity (Eq. (12)) can be directly used as an extra dipole strength in the evaluation of γ decay in the CN evaporation cascade. From the detailed balance we have a statistical γ-emission rate, for each dipole component,

$$R_\gamma(E_\gamma) = \frac{\rho(E^* - E_\gamma)}{\rho(E^*)} \frac{\sigma_{\mathrm{abs}}(E_\gamma)}{3} \frac{E_\gamma^2}{(\pi\hbar c)^2} =$$

$$= \frac{\rho(E^* - E_{\mathrm{GDR}})}{\rho(E^*)} \Big[\frac{\rho(E^* - E_\gamma)}{\rho(E^* - E_{\mathrm{GDR}})} \frac{\sigma_{\mathrm{abs}}(E_\gamma)}{3} \frac{E_\gamma^2}{(\pi\hbar c)^2} \Big], \tag{14}$$

where $\sigma_{\mathrm{abs}}(E_\gamma)$ is the γ-dipole absorption cross section. This leads, for the component with pre-equilibrium contribution, along the symmetry axis, to a time dependent quantity

$$R_\gamma(E_\gamma, t) = n_{\mathrm{GDR}}(t) \Big[\frac{\rho(E^* - E_\gamma)}{\rho(E^* - E_{\mathrm{GDR}})} \frac{\sigma_{\mathrm{abs}}(E_\gamma)}{3} \frac{E_\gamma^2}{(\pi\hbar c)^2} \Big] \tag{15}$$

with $n_{\mathrm{GDR}}(t)$ given by Eq. (12).

The final yield of photons emitted can be then evaluated using a time-dependent evaporation cascade procedure, see Ref. 50. From Eqs. (15) and (12) once fixed the CN initial excitation energy (temperature) the results will be critically dependent on $n^{(0)}_{\rm GDR}$ and $\Gamma^{\downarrow}(T)$.

To show how the method is working and the sensitivity to the above parameters in Fig. 6 we report some results for the systems studied by Flibotte et al. [27]. The curves represent the «subtracted» photon spectra (*i.e.*, normalized to a statistical emission without GDR): in Fig. 6*a* the data for the two systems, $\mathrm{Ca} + \mathrm{Mo}$ (charge asymmetric, dashed) and $\mathrm{S} + \mathrm{Pd}$ (more symmetric, solid), and in Figs. 6*b,c,d* the results obtained from 10^5 runs of a Monte-Carlo evaporation cascade [49, 50] with the same initial conditions for the CN and varying only $n^{(0)}_{\rm GDR}$ and $\Gamma^{\downarrow}(T)$. The best results (Fig. 6*b*) are obtained with the values $n^{(0)}_{\rm GDR} = 0.14$ and $\Gamma^{\downarrow} = 8$ MeV. Now while it is reasonable to have a GDR-damping width larger than in the ground state of the same compound nucleus Sm^{140} (4.8 MeV used in Fig. 6*c*) the choice of $n^{(0)}_{\rm GDR}$ requires a deeper dynamical justification. This is the aim of the next section, where we will also look at the beam energy dependence of this GDR extra strength.

THE INTERPLAY BETWEEN FUSION DYNAMICS AND PRE-EQUILIBRIUM GDR

In this section we present a fully microscopic analysis of the fusion reaction for some systems of interest, to look in particular at the pre-equilibrium GDR population. The calculations are performed in the framework of the BNV transport equation which incorporates in a self-consistent way the mean field and two-body collisions dynamics [59]. The numerical accuracy has been largely improved in order to have a good description also of low energy fusion reactions, see discussion in [57]. For the mean field we have adopted a Skyrme-like parametrization, as described in [57], which well reproduces Nuclear Matter saturation properties (equilibrium density, binding energy, compressibility, and symmetry energy). In the collision integral we use in medium reduced nucleon–nucleon cross sections, isospin as well as energy and angular dependent [48].

We have focussed our attention on the fusion reaction induced by $^{16}\mathrm{O}$ $(N/Z = 1)$ on $^{98}\mathrm{Mo}$ $(N/Z = 1.33)$ (see [28]). We have studied in a relative large range of incident beam energy, at 4 MeV/n, 8 MeV/n, 14 MeV/n and 20 MeV/n, the evolution of the composite system along the fusion path. We will consider results that correspond to an impact parameter $b = 0$ as well representative of the features we are looking for.

In all plots we choose as $t = 0$ the time corresponding to the «touching» configuration. As discussed in the previous section this can be considered the starting

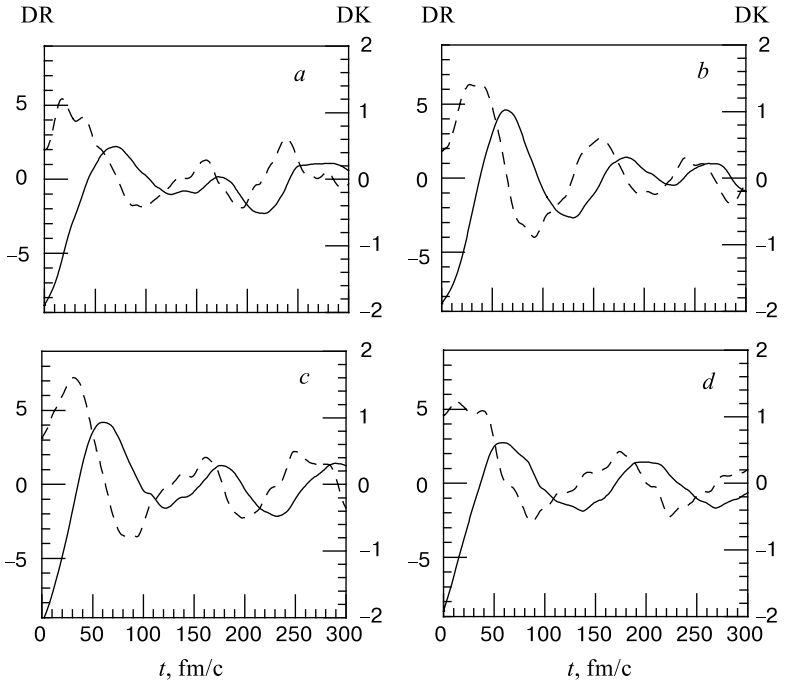

Fig. 7. Time evolution of the dipole moment in r-space, DR (solid lines, left scales) and in p-space, DK (dashed lines, right scales) for the $\mathrm{O} + \mathrm{Mo}$ system at beam energies: a) $4\,A$ MeV, b) $8\,A$ MeV, c) $14\,A$ MeV, d) $20\,A$ MeV. $t = 0$ corresponds to the touching configuration (see text)

time of phase II, when charge equilibration and the relative collective dipole are present in the dinuclear system. In fact this point can be checked from simulations, see later.

At each time step we can evaluate the dinuclear dipole moment in coordinate and momentum space:

$$DR(t) = \frac{NZ}{A} X(t), \tag{16}$$

$$DK(t) = \frac{\Pi(t)}{\hbar}. \tag{17}$$

The results are shown in Fig. 7. The out-of-phase behaviour of the two dipoles, clear signature of a collective dinuclear response, is actually starting just after $t = 0$ (touching configuration) practically for all energies. We remark a smaller initial amplitude of the oscillation at the lowest ($4\,A$ MeV) and highest ($20\,A$ MeV) energies, as well as an increase of the damping with the beam energy. In conclu-

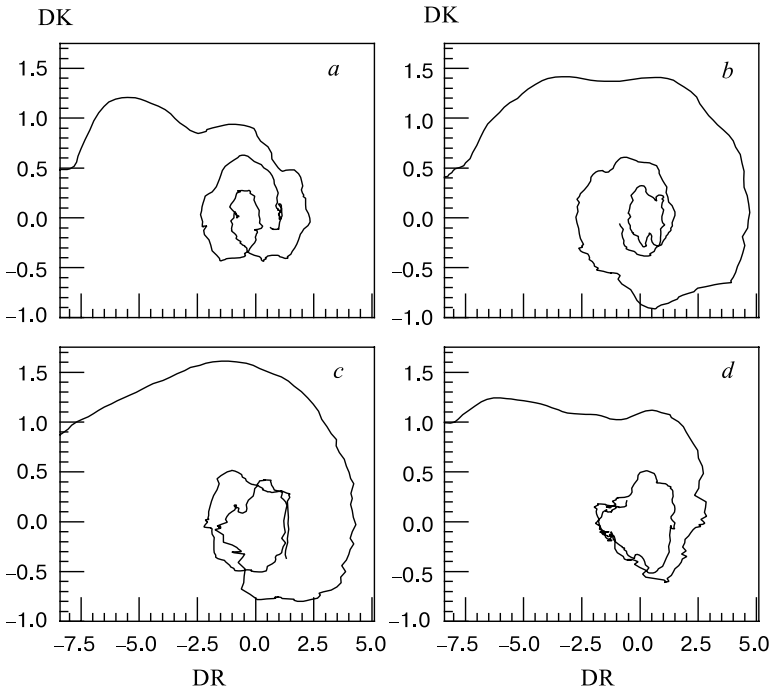

Fig. 8. Phase space trajectory of the entrance channel dipole for the $\mathrm{O} + \mathrm{Mo}$ reaction. The labels correspond to the same energies of Fig. 7

sion it clearly appears an optimum range of energies for the observation of the dynamical dipole effect, well above the Coulomb threshold (about $4\,A$ MeV in the $\mathrm{O} + \mathrm{Mo}$ system) but also well below the Fermi energy domain. This point will be further analysed in the following.

Figure 8 shows phase-space trajectories of the GDR, *i.e.*, the time evolution of the $DK - DR$ correlation. The spiral curves are nicely revealing an out-of-phase behaviour in presence of some damping. The spiralling trend seems to start at the touching configuration ($t = 0$, left points of the curves), maybe with some delay in the lowest energy case. The centre is reached when the CN formation is achieved. The spiral quickly collapses to the central region at high beam energy (Fig. 8*d*) since we have a larger damping of the collective motion, as already seen in Fig. 7.

The amplitude reduction at $4\,A$ MeV and $20\,A$ MeV is also evident: the nature of the effect is however different in the two cases. At low energy, just above the Coulomb barrier, the neck is formed quite slowly (see Fig. 9) and so the collective dipole response of the dinuclear system is actually starting sometimes after the

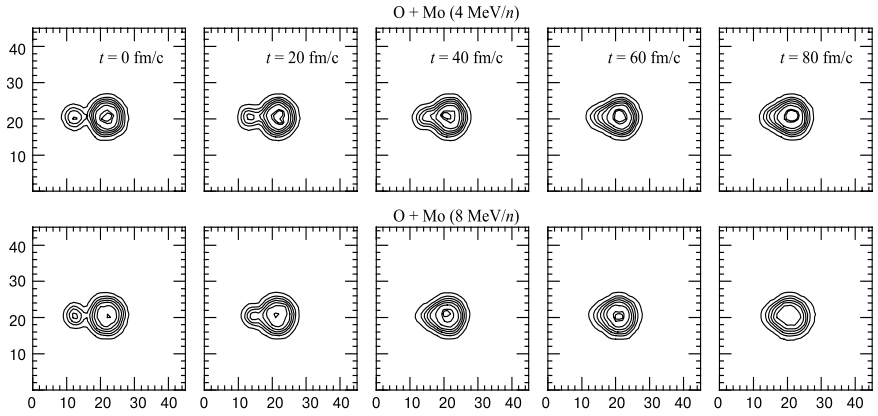

Fig. 9. Density plots of the neck dynamics for the O + Mo system at the two energies 4 A MeV and 8 A MeV

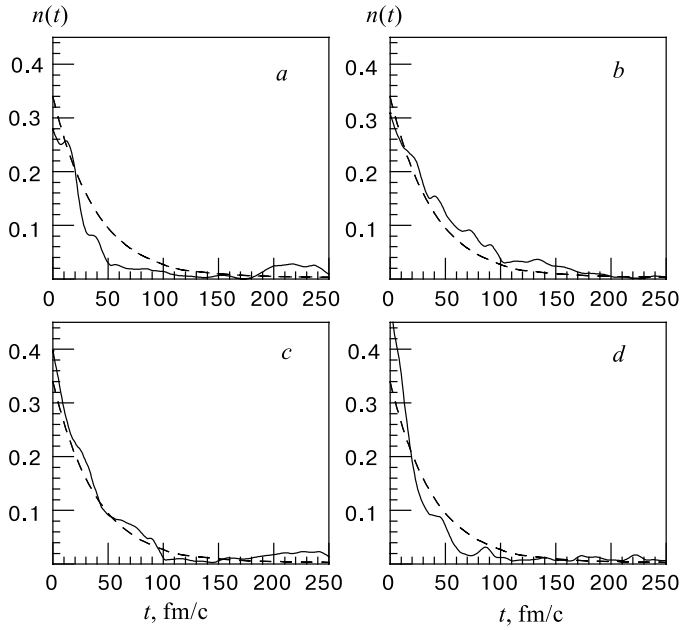

Fig. 10. Time evolution of the number of dipole phonons for the O + Mo reaction (solid lines). The labels correspond to the same energies of Fig. 7. The dashed line is the reference curve discussed in the text

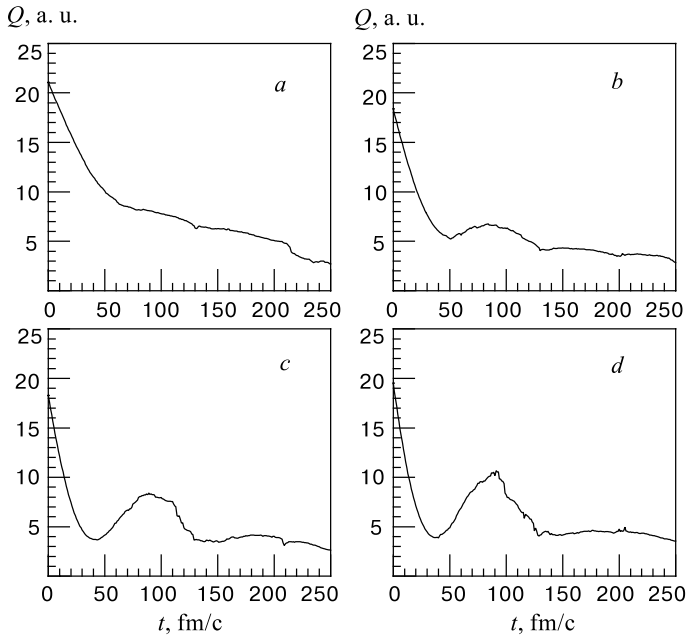

Fig. 11. Time evolution of the mass quadrupole moment for the $\mathrm{O} + \mathrm{Mo}$ reaction. The labels correspond to the same energies of Fig. 7

touching configuration, when some charge equilibration has already taken place. At $20\,A$ MeV the fusion dynamics is fast but now we can have some prompt particle emission that will reduce the dipole moment of the dinucleus. Just by chance we see the best spiralling behaviour at $8\,A$ MeV, where the experiment has been performed by Cinausero et al. [28] with a very clear evidence of the dynamical dipole enhancement.

Now we can dynamically evaluate the number of pre-equilibrium GDR-phonons $n^{(0)}_{\mathrm{GDR}}$ present at the time of CN formation: as shown in the previous section this quantity is essentially ruling the extra emission of GDR γ rays. At each time step the average number of phonons $n(t)$ can be determined from the simulations just dividing the total oscillator energy, as defined by Eq. (5), by the one phonon energy at that instant, $\hbar\omega(t)$, *i.e.*, corresponding to the deformation at the time t. The results are presented in Fig. 10. The dashed curve in all four pictures is the analytical prediction of Eqs. (4) and (7) using a constant spreading width value, $\Gamma^{\downarrow} = 5$ MeV. We remark a quite good overall agreement at beam energies 8 MeV/n and 14 MeV/n, although with increasing energy we see a higher starting point joint to a faster damping. This is particularly evident at 20 MeV/n (Fig. 10*d*), where we have to consider a larger value for the spreading width and the kinetic term contribution to the initial number of phonons n_i.

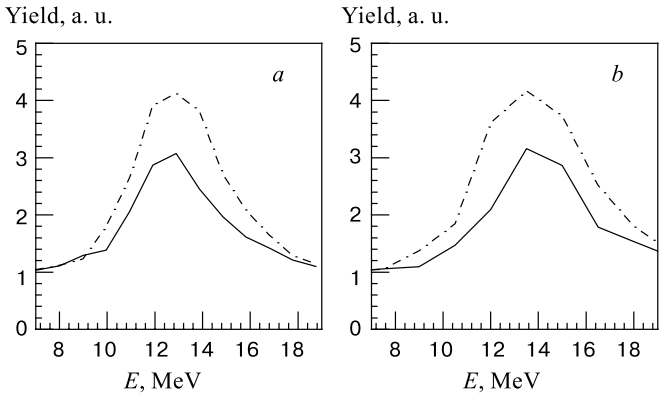

Fig. 12. Subtracted γ spectra from a $^{114}\mathrm{Sn}$ CN formed at $E^* = 108$ MeV in the charge asymmetric ($\mathrm{O} + \mathrm{Mo}$ — dashed lines) and symmetric ($\mathrm{Ti} + \mathrm{Ni}$ — solid lines) entrance channel: *a*) experiment [28]; *b*) simulations (see text) with $(n^{(0)}_{\mathrm{GDR}}, \Gamma^{\downarrow})$ respectively equal to (0.07, 7 MeV). $2 * 10^5$ Montecarlo events

The quantity we are loking for, $n^{(0)}_{\mathrm{GDR}}$, is now given by the value of $n(t)$ at the time of Compound Nucleus formation t_{CN}, Eq. (10). In Fig. 11 we plot the time evolution of the mass quadrupole moment in real space at the four incident energies. Generally we remark two distinct behaviours in the evolution: a faster decay until the first minimum is reached, followed by a smoother trend accompanied by small oscillations. During the first stage the conversion of relative motion in heat takes place and therefore, in the limits of some more time needed for a final thermal equilibration, the moment when the first minimum is attained will provide us the Compound Nucleus formation time. Our evaluation is in agreement with the information obtained by looking at the quadrupole in momentum space. We can extract t_{CN} values of 120 fm/c at $4\,A$ MeV, 80 fm/c at $8\,A$ MeV, and 50 fm/c at the higher energies $14\,A$ MeV and $20\,A$ MeV. From Fig. 10 we get the corresponding $n^{(0)}_{\mathrm{GDR}} = n(t_{\mathrm{CN}})$ parameters: 0.01 at $4\,A$ MeV going up to 0.07 at $8\,A$ MeV and 0.08 at $14\,A$ MeV and finally reducing again, around 0.05, at $20\,A$ MeV.

To test the correctness of our procedure we have performed a complete evaporation cascade calculation using the above extra dipole strength for the system $\mathrm{O} + \mathrm{Mo}$ at $8\,A$ MeV. The subtracted spectra are shown in Fig. 12, from $2 * 10^5$ Monte-Carlo events, compared with experimental data from Ref. 28. The agreement is quite good.

Since the time scale of fusion dynamics is playing an important role on the amount of extra dipole strength present at the time of CN formation we expect to see some dependence of the effect also on the mass symmetry in

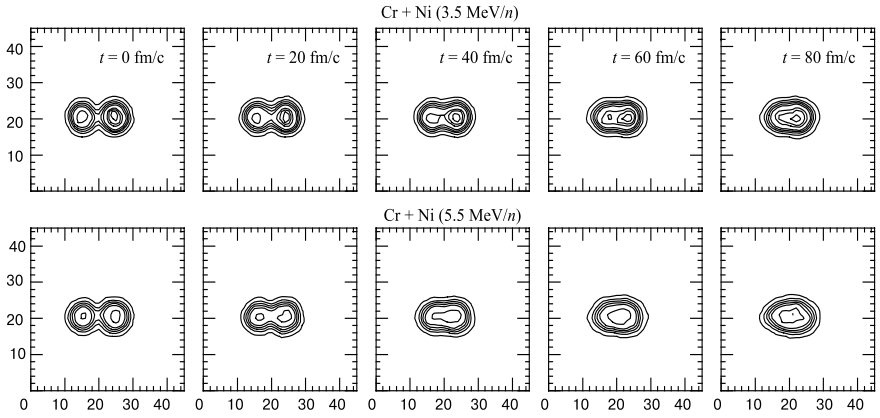

Fig. 13. Density plots of the neck dynamics for the $\mathrm{Cr} + \mathrm{Ni}$ system at the two energies 3.5 A MeV and 5.5 A MeV

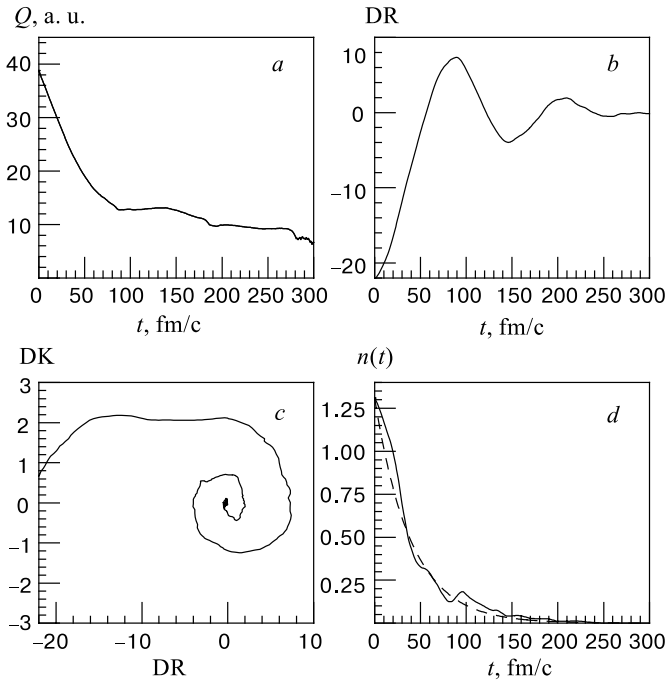

Fig. 14. Time evolution of mass quadrupole moment (a), r-dipole moment (b), p-dipole moment (c) and average number of dipole phonons (d) for the reaction $\mathrm{Ca} + \mathrm{Mo}$ at 4 A MeV

the entrance channel, which is strongly affecting the fusion time, see [50] and refs. therein. In order to check this point we have studied the system $^{50}\mathrm{Cr}$ ($N/Z = 1.08$) + $^{64}\mathrm{Ni}$ ($N/Z = 1.28$) with almost the same charge asymmetry of $\mathrm{O} + \mathrm{Mo}$ but much more symmetric in mass. We have considered the beam energies 3.5 and 5.5 A MeV corresponding to the same c.m energies above the Coulomb barrier of the first two cases of the $\mathrm{O} + \mathrm{Mo}$ system. The relative fusion paths are shown in Fig. 13 for 100 fm/c starting from the touching configuration, to be compared with the equivalent Fig. 9 of the $\mathrm{O} + \mathrm{Mo}$. At both energies it is quite evident the longer neck formation and shape equilibration times. As discussed before we expect a smaller initial amplitude for the collective dipole oscillation (neck dynamics) and a further reduction due to the delay in the CN formation (shape dynamics).

We have finally checked the method also for the Ref. 27 system, $\mathrm{Ca} + \mathrm{Mo}$ at 4 A MeV, where the best results are obtained with a $n^{(0)}_{\mathrm{GDR}} = 0.14$, see Fig. 6. In Fig.14 we present the time evolution of the relevant quantities, mass quadrupole moment, dipole moments in r- and p-space and average number of phonons. We see a slower fusion process but with a larger initial dipole strength. We have a $t_{\mathrm{CN}} \simeq 120$ fm/c and a corresponding $n^{(0)}_{\mathrm{GDR}}$ ranging between 0.12 and 0.15, as needed in the fitting procedure of Fig. 6.

SUMMARY AND CONCLUSIONS

We have studied the isovector response of a heated nuclear matter in the framework of the Landau–Fermi liquid theory with a Skyrme-like mean field and a collision integral in the relaxation time approximation. The ultimate goal is to recognize if, in the isovector motion at finite temperature, the hydrodynamic regime (first-sound) switches on, or a pure mean field one-body propagation (zero-sound) remains valid at all temperatures where the GDR mode exists. A related question is to predict experimental signatures of the transition in hot nuclei.

The relaxation times of the perturbations with various multipolarities in momentum space are calculated starting from the Boltzmann–Uehling–Uhlenbeck collision integrals with energy and angular dependent differential NN scattering cross sections. In the application to finite nuclear systems, the main difficulty is the choice of these cross sections. Two cases are considered here, which give some upper and lower *theoretical* limits for the collisional damping of the GDR mode in a heavy spherical nucleus: vacuum cross sections, and in-medium reduced cross sections calculated at the nuclear saturation density within the Dirac–Brueckner approach based on the Bonn A potential (see Refs. 48) in cold nuclear matter.

The photoabsorption cross section by a heated nucleus has been derived using the Steinwedel–Jensen model. The calculations of γ spectra from a thermally

excited nucleus ^{208}Pb at $E^* = 45$ and 100 MeV have been performed on the basis of the statistical model MONTECASCA of Ref. 49, 50 with theoretical photoabsorption cross sections included at each step of the decay chain. The agreement with the experimental data of Ref. 13 is much better when vacuum NN cross sections are used in the calculation of the photoabsorption strength, rather than the in-medium reduced ones. The same conclusion was reached in Ref. 8 for the case of an excited nucleus ^{120}Sn.

In general from all these studies it seems that with increasing temperature a collisional damping larger than the one given by in-medium reduced cross sections is required. We can have some hints to understand this effect:

1) The Dirac–Brueckner calculations of Ref. 48 have been performed in cold NM. With increasing temperature the blocking factor for intermediate states is reduced and the scattering matrix should be closer to the free one. Moreover some correlation contributions to the particle propagator are also decreasing and the effective mass will approach the bare mass value. Some very recent results seem to confirm this trend [60].

2) At high temperature we can have a thermal expansion of the system and medium effects on NN cross sections should be evaluated at lower mean densities.

3) All the analytical methods used to calculate relaxation times are based on a Pauli Blocking frozen at the initial momentum space occupation. A rearrangement of the blocking on the way to equilibrium is also acting in the direction of shortening the final relaxation times [61].

The present study has shown that in a heavy nucleus like ^{208}Pb:

(i) The isovector volume mode is a zero sound mode at temperatures $T \leq 4$ MeV. At higher temperatures it becomes a first sound mode strongly damped by the friction force between the neutron and proton liquids.

(ii) The energy of the mode decreases slightly by about 1 MeV as the temperature increases from 0 to 5 MeV. At higher temperatures the energy quickly tends to zero and the mode disappears at $T \sim 7$ MeV due to strong interflow friction.

(iii) The GDR damping increases monotonically with temperature. At low (high) temperatures the width increase is determined mostly by the τ_2 (τ_1) relaxation time.

(iv) The Lorentzian shape of the photoabsorption cross section at high temperatures is a consequence of a first-sound (hydrodynamic) isovector collective motion. At low temperatures, in the zero-sound regime, the shape is not Lorentzian. Due to the absence of the shell structure in our model, which is important at $T \leq 1 - 2$ MeV, the last conclusion has to be taken with a caution. However, if for some spherical nucleus the photoabsorption cross section is not Lorentzian at the ground state, the Lorentzian shape will be restored with increasing temperature.

A zero-to-first sound transition is found for the isovector volume mode in $^{208}\mathrm{Pb}$ at temperature $T_{tr} \simeq 4.5$ MeV. Moreover from the simple condition $\omega_R \tau_2 \simeq 1$ we can estimate a $A^{-1/6}$ mass dependence of T_{tr}: $T_{\mathrm{tr}} \sim \sqrt{k_{\mathrm{GDR}}(A)} \sim$ $\sim R^{-1/2}$. Therefore an experimental confirmation of this transition requires to create a dipole vibration in an extremely hot nucleus, close to maximum temperature that nuclei can sustain. This can be reached in heavy ion collisions, although with some difficulties [5, 6]. Further detailed comparisons of the present model with the data on γ emissions from hot nuclei are necessary.

In the second part of this report we have shown that important information on the early stage of the fusion path can be obtained studying charge-asymmetric reactions. In fact, in this case it is possible to reveal a «direct» dipole oscillations (*the dynamical dipole*), related to the charge-equilibration dynamics, which leads to some extra GDR strength in the statistical decay of the fused system. In this work we have investigated how N/Z asymmetry and fusion dynamics are affecting the properties of the pre-equilibrium GDR remnants. We have shown the existence of a GDR collective mode, during the formation phase of the compound nucleus, *i.e.*, built on nonequilibrium states. This has allowed us to express the mean number of dipole phonons present in the fused nucleus in terms of the initial isospin asymmetry, CN formation time and GDR spreading width. We can make quite accurate predictions on the optimal choice of the reaction partners, in particular on the interplay between charge and mass asymmetry in the entrance channel.

Particularly interesting is to follow the energy dependence of the effect. We expect to see a *rise and fall* of the dynamical dipole contribution.

At low energies, just above the Coulomb barrier, the effect is strongly reduced for two combined reasons:

- i) A delay in the dinucleus formation (slow neck dynamics) and relative collective response. The pre-equilibrium dipole oscillation of the composite system will have an initial smaller amplitude since some charge equilibration has already taken place.
- ii) A longer Compound Nucleus formation time is decreasing the average number of phonons present in the fused system due to the GDR damping.

At higher energies, close to the Fermi energy domain, the effect is again reduced on average for two main reasons:

- i) We have a relevant pre-equilibrium particle emission (*i.e.*, incomplete fusion events) with a direct reduction of the initial charge asymmetry.
- ii) In the fusion processes we have a large excitation energy deposited in the composite system with a related increase of the GDR spreading width leading to a fast decrease of the number of dipole phonons.

Moreover a new dynamical feature is appearing at energies above 20 A MeV, some large monopole oscillations in the entrance channel dynamics [5,6,62]. The dynamical dipole strength is reduced and more fragmented, see the simulations in Ref. 62, although still present as confirmed from very recent data [32, 33]. The study of the dynamical dipole effect in the Fermi energy domain, although experimentally quite difficult, would therefore bring new independent information on the spreading width of hot GDR and in particular on the coupling to an expanding collective mode.

Moreover, for charge asymmetric reactions, the enhanced dipole emission could be an interesting cooling mechanism to favour the fusion of very heavy nuclear systems. From the interplay between charge and shape equilibration time-scales we can also suggest new experiments to study the dipole propagation in excited nuclei. The use of radioactive beams will enhance the possibility of such observations.

ACKNOWLEDGEMENTS

We warmly thank D.M.Brink and Ph.Chomaz for many pleasant and enlightening discussions. We are deeply grateful to the TRASMA experimental group of LNS-Catania, in particular to F.Amorini, G.Cardella, M.Papa, and S.Tudisco for the availability of their «fresh» data and for a stimulating interface. Three of us (V.B., A.B.L., and N.T.) acknowledge the INFN support for their stay at the Laboratori Nazionali del Sud, Catania. They also deeply thank the LNS staff for the warm atmosphere and the good working conditions.

REFERENCES

1. **Van der Woude A.** — Nucl. Phys., 1996, v.A599, p.393c.
2. **Brink D.M.** — Nucl. Phys., 1990, v.A519, p.3c.
3. **Snover K.A.** — Annu. Rev. Nucl. Part. Sci., 1986, v.36, p.545.
4. **Gaardhoje J.J.** — Annu. Rev. Nucl. Part. Sci., 1992, v.42, p.483.
5. **Piattelli P. et al.** — Nucl. Phys., 1999, v.A649, p.181c.
6. **Suomijarvi T.** — RIKEN Symp. on Dynamics in Hot Nuclei, 1998, p.1.
7. **Baran V. et al.** — Nucl. Phys., 1996, v.A599, p.29c.
8. **Thoennessen M. et al.** — Nucl. Phys., 1998, v.A649, p.173c;
   Gervais G., Thoennessen M., Ormand W.E. — Phys. Rev., 1998, v.C58, p.R1377.
9. **Snover K.A. et al.** — RIKEN Review, 1999, v.23, p.111,
   Kelly M.P. et al. — Phys. Rev. Lett., 1999, v.82, p.3404.
10. **Snover K.A. et al.** — Nucl. Phys., 1998, v.A649, p.130c.
11. Proc. Giant Resonance Conf., Groningen 1996, Nucl. Phys., 1996, v.A599.

12. **Baumann T., Ramakrishnan E., Thoennessen M.** — Acta Physica Polonica, 1997, v.B29, p.197 and refs. therein.

13. **Baumann T. et al.** — Nucl. Phys., 1998, v.A635, p.428.

14. **Thoennessen M. et al.** — RIKEN Review, 1999, v.23, p.132.

15. **Kondratyev V.N., Di Toro M.,** — Phys. Rev., 1996, v.C53, p.2176.

16. **Baran V. et al.** — Progr. Part. Nucl. Phys., 1997, v.38, p.263.

17. **Abel W.R., Anderson A.C., Weathley J.C.** — Phys. Rev. Lett., 1966, v.17, p.74.

18. **Landau L.D.** — Soviet Phys. JETP, 1957, v.5, p.101;
Lifshitz E.M., Pitaevskii L.P. — «Physical Kinetics», Pergamon Press, 1993.

19. **Abrikosov A.A., Khalatnikov I.M.** — Rep. Progr. Phys., 1959, v.22, p.329.

20. **Bertsch G.F.** — Nucl. Phys., 1975, v.A249, p.253; Zeit. Phys., 1978, v.A289, p.103.

21. **Wilczynski J. et al.** — Phys. Rev., 1996, v.C54, p.325.

22. **Paul P.** — Nucl. Phys., 1998, v.A630, p.92c.

23. **Baran V. et al.** — Journ. of Phys. G: Nucl. Part. Phys., 1997, v.23, p.1341.

24. **Larionov A.B., Piperova J., Colonna M., Di Toro M.** — Strongly Damped Nuclear Collisions: Zero or First Sound?, Preprint LNS, Dec. 1999, sub. Phys. Rev. C.

25. **Chomaz Ph.** — In: Proceedings of the 6th Franco-Japanese Colloquium, St. Malo, France, 1992, edited by N.Alamanos, S.Fortier and F.Dykstra, Saclay, 1993.

26. **Chomaz Ph., Di Toro M., Smerzi A.** — Nucl. Phys., 1993, v.A563, p.509.

27. **Flibotte S. et al.** — Phys. Rev. Lett., 1996, v.77, p.1448.

28. **Cinausero M. et al.** — Nuovo Cimento, 1998, v.A111, p.613.

29. **Amorini F. et al.** — Phys. Rev., 1998, v.C58, p.987.

30. **Trotta M. et al.** — RIKEN Review, 1999, v.23, p.96;
Sandoli M. et al. — Eur. Phys. J., 1999, v.A6, p.275.

31. **Papa M. et al.** — Eur. Phys. J., 1999, v.A4, p.69.

32. **Amorini F.** — TRASMA exp., Ph.D.Thesis LNS, Catania, 1998.

33. **Tudisco S.** — TRASMA exp., Ph.D.Thesis LNS, Catania, 1999.

34. **Kolomietz V.M., Larionov A.B., Di Toro M.** — Nucl. Phys., 1997, v.A613, p.1.

35. **Migdal A.B.** — Theory of Finite Fermi Systems and Applications to Atomic Nuclei, Interscience, London 1967.

36. **Heiselberg H., Pethick C.J., Ravenhall D.G.** — Ann. Phys. (N.Y.), 1993, v.223, p.37 and refs. therein.

37. **Baran V. et al.** — Nucl. Phys., 1999, v.A649, p.185c.

38. **Larionov A.B., Cabibbo M., Baran V., Di Toro M.,** — Nucl. Phys., 1999, v.A648, p.157.

39. **Pines D., Nozieres P.** — The Theory of Quantum Liquids. Benjamin, New York, 1966, v.1.

40. **Hofmann H., Yamaji S., Jensen A.S.** — Phys. Lett., 1992, v.B286, p.1;
Yamaji S., Jensen A.S., Hofmann H. — Prog. Theor. Phys., 1994, v.92, p.773.

41. **Braghin F.L., Vautherin D.** — Phys. Lett., 1995, v.B333, p.289,
Braghin F.L., Vautherin D., Abada A. — Phys. Rev., 1995, v.C52, p.2504.

42. **Di Toro M., Kolomietz V.M., Larionov A.B.** — Proc. Dubna Conf. on Heavy Ion Physics, World Sci., 1998, p.285; Phys. Rev., 1999, v.C59, p.3099.

43. **Ring P., Schuck P.** — The Nuclear Many-Body Problem. Springer-Verlag, New-York, 1980.

44. **Eisenberg J.M., Greiner W.** — Nuclear Models. North Holland, 1987, pp.606, 626.

45. **Ayik S., Boilley D.** — Phys. Lett., 1992, v.B276, p.263; 1982, v.B284, p.482,
Ayik S., Yilmaz O., Gokalp A., Schuck P. — Phys. Rev., 1998, v.C58, p.1594.

46. **Kolomietz V.M., Plujko V.A., Shlomo S.** — Phys. Rev., 1996, v.C54, p.3014 and refs. therein.

47. **Plujko V.A.** — Acta Phys. Pol., 1999, v.30, p.1383.

48. **Li G.Q., Machleidt R.** — Phys. Rev., 1993, v.C48, p.1702; Phys. Rev., 1994, v.C49, p.566;
Li G.Q. — private communications.

49. **Cabibbo M.** — MONTECASCA Code, Ph.D. Thesis, Univ. of Catania, 1998.

50. **Cabibbo M., Baran V., Colonna M., Di Toro M.** — Nucl. Phys., 1998, v.A637, p.374.

51. **Morsch H.P. et al.** — Phys. Rev. Lett., 1990, v.64, p.1999.

52. **Gregoire C.** — In: Proceedings of the Winter College on Fundamental Nuclear Physics, v.1, Trieste, Italy, 1984, edited by K.Dietrich, M.Di Toro, H.J.Mang, p.497.

53. **Hofmann H. et al.** — Z. Physik, 1979, v.A293, p.229.

54. **Bonche P., Ngo N.** — Phys. Lett., 1981, v.B105, p.17.

55. **Suraud E., Pi M., Schuck P.** — Nucl. Phys., 1988, v.A482, p.187c.

56. **Suraud E., Pi M., Schuck P.** — Nucl. Phys., 1989, v.A492, p.294.

57. **Baran V. et al.** — Nucl. Phys., 1996, v.A600, p.111.

58. **Brink D.M.** — D.Phil. Thesis, Oxford, 1955.
Axel P. — Phys. Rev., 1962, v.126, p.671.

59. **Bonasera A. et al.** — Phys. Lett., 1989, v.B221, p.233;
Bonasera A. et al. — Phys. Rep., 1994, v.243, p.1.

60. **Schnell A., Röpke G., Lombardo U., Schulze H.J.** — Phys. Rev., 1998, v.C57, p.503.

61. **Bonasera A., Di Toro M., Gulminelli F.** — Phys. Rev., 1990, v.C42, p.966.

62. **Di Toro M. et al.** — Acta Phys. Polonica, 1999, v.B30, p.1331.